Modeling of light-induced defect creation in hydrogenated amorphous silicon

K. Morigaki[1,*] and H. Hikita[2,†]
[1]*Department of Electrical and Digital-System Engineering, Hiroshima Institute of Technology, Miyake, Saeki-ku, Hiroshima 731-5193, Japan*
[2]*Physics Laboratory, Meikai University, Urayasu, Chiba 279-8550, Japan*
(Received 10 July 2006; revised manuscript received 18 December 2006; published 2 August 2007)

Light-induced defect creation in hydrogenated amorphous silicon (*a*-Si:H) is discussed in terms of a model based on the breaking of weak Si–Si bonds by self-trapping of holes under illumination. In this model, two separate dangling bonds, i.e., a normal dangling bond and a hydrogen-related dangling bond that is a dangling bond having hydrogen at a nearby site, are created under illumination. Further, we take into account dissociation of hydrogen atoms from hydrogen-related dangling bonds, termination of two types of dangling bonds by dissociated hydrogen atoms (metastable hydrogen atoms), insertion of dissociated hydrogen atoms into nearby weak Si–Si bonds, and formation of hydrogen molecules by collision of dissociated hydrogen atoms. Taking into account these processes, rate equations governing the kinetics of two types of dangling bonds and metastable hydrogen atoms under illumination are numerically solved for the case of continuous illumination. The calculated results are compared with experimental results taken from literature. Furthermore, we discuss the case of low-temperature illumination, the kinetics of light-induced dangling bonds given by stretched exponential function, and saturated density of light-induced dangling bonds in *a*-Si:H.

DOI: 10.1103/PhysRevB.76.085201 PACS number(s): 73.61.Jc, 71.55.Jv

I. INTRODUCTION

The Staebler-Wronski effect[1] that band gap illumination on hydrogenated amorphous silicon (*a*-Si:H) causes photoconductivity and dark conductivity to decrease with 1 order of magnitude and 3 orders of magnitudes, respectively, compared to those in the dark has been elucidated for the last three decades. This effect has been clarified to be associated with light-induced creation of dangling bonds, but the mechanism for light-induced creation of dangling bonds is still a controversial issue. Until now, a number of models for light-induced defect creation in *a*-Si:H have been reported on the basis of breaking of weak Si–Si bonds under illumination.[2–8] Other models based on charged defects and/or impurities have also been reported so far.[2–8]

In the following, we summarize the models based on breaking of weak Si–Si bonds under illumination. Hirabayashi *et al.*[9] pointed out for the first time that a weak Si–Si bond adjacent to a Si–H bond may be broken under illumination, while Pankove and Berkeyheiser[10] suggested that a weak Si–Si bond located far from Si–H bonds may be broken under illumination. After then, Dersch *et al.*[11] pointed out that after weak-bond breaking, the Si–H bond switches toward the broken weak Si–Si bond to stabilize light-induced two close dangling bonds. Stutzmann *et al.*[12] developed further this weak-bond breaking model using rate equations and compared between theory and experiment on the illumination-time dependence of light-induced dangling bond density with good agreement. In models of Dersch *et al.*[11] and Stutzmann *et al.*,[12] a weak Si–Si bond adjacent to a Si–H bond is broken under illumination as a result of nonradiative electron-hole pair recombination in the weak Si–Si bond. As mentioned above, Hirabayashi *et al.*[9] suggested that a Si–Si bond adjacent to a Si–H bond becomes weak on the basis of considerations on differences in bond strength between the Si–Si bond and the Si–H bond and in electronegativity between Si and H atoms. This has been demonstrated by *ab initio* molecular dynamics computer simulations by Yonezawa *et al.*[13] that this is the case in *a*-Si:H. Morigaki[14] showed that two close dangling bonds created by a weak-bond breaking are separated by further Si–H bond switching and H hopping and tunneling, and eventually two types of dangling bonds, i.e., a normal dangling bond and a dangling bond having hydrogen at a nearby site, so-called hydrogen-related dangling bond, are formed. Further, he[15–17] developed this model taking into account self-trapping of a hole in a weak Si–Si bond adjacent to a Si–H bond and nonradiative recombination of this hole with an electron, triggering the weak-bond breaking, as described above, and considered the temperature dependence of light-induced dangling bond density in *a*-Si:H. Recently, this model has been extended[18–22] by taking into account dissociation of hydrogen atoms from Si–H bonds located nearby hydrogen-related dangling bonds as a result of nonradiative recombination of electrons and holes in the hydrogen-related dangling bonds, the termination of normal dangling bonds and hydrogen-related dangling bonds by these dissociated hydrogen atoms, i.e., metastable hydrogen atoms, and the insertion of these metastable hydrogen atoms into nearby weak Si–Si bonds in *a*-Si:H.

A breaking of a Si–H bond by hole trapping was first suggested by Carlson,[23] particularly in the Si:H bonds on internal surfaces of microvoids. He also suggested that after a Si–H bond is broken, the hydrogen atom moves to a nearby weak Si–Si bond and breaks it and the resulting dangling bonds reconstruct aided by the trapping of an electron. Further, a breaking of a Si–H bond in the $(\text{Si-H})_2$ configuration and in the single Si–H configuration associated with nonradiative electron-hole pair recombination has been postrated, respectively, by Godet and Roca i Cabarrocas[24] and Godet,[25,26] and by Branz.[27–30] Godet and Roca i Cabarrocas[24] and Godet[25] considered hydrogen movements through three-center bonds, while Branz[27–30] considered them through

 ©2007 The American Physical Society

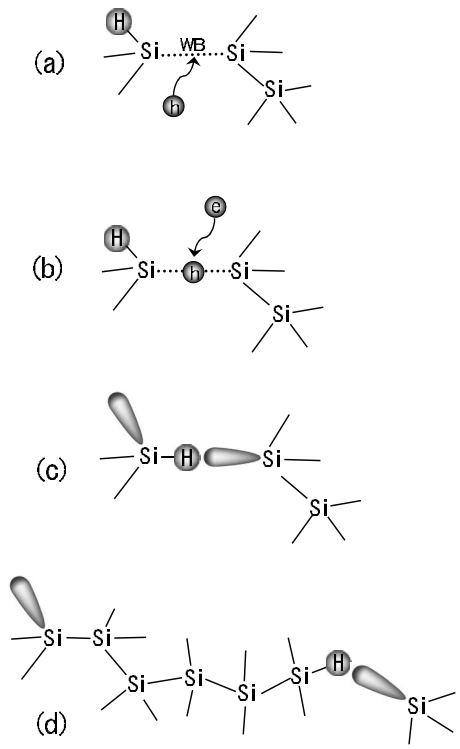

FIG. 1. Atomic configurations involved in the formation of two types of dangling bonds, i.e., normal dangling bonds and hydrogen-related dangling bonds, under illumination: (a) self-trapping of a hole in a weak Si-Si bond (WB) adjacent to a Si-H bond, (b) electron-hole recombination at a weak Si-Si bond, (c) switching of a Si-H bond toward the weak Si-Si bond, leaving a dangling bond behind, and (d) formation of two separate dangling bonds after hydrogen movements and repeating of processes shown in (a)–(c).

Si–H bond-dangling bond complexes as well as their collision. Recently, Longeaud *et al.*[31] proposed a model in which a local configuration containing two Si–H bonds and an interstitial hydrogen molecule transforms to other configuration containing two dangling bonds and two interstitial hydrogen molecules through intermediate stages involving hydrogen in the bond-center (BC) site or the antibonding site after breaking of Si–H bonds as a result of nonradiative electron-hole pair recombination.

In this paper, we present a detailed account of our model along with comparisons with experimental results of light-induced creation of dangling bonds at room temperature as well as at low temperatures under continuous illumination. We have already reported in Refs. 21, 22, and 32 the case of intense pulsed illumination.

II. MODEL

A new model[18–22] for light-induced defect creation in *a*-Si:H, extending a previous model,[14–17] takes into account the following processes: After a hole is self-trapped in a weak Si–Si bond adjacent to a Si–H bond [Fig. 1(a)], the weak bond is broken as a result of nonradiative recombination between an electron and a self-trapped hole [Fig. 1(b)]. Followed by switching of the Si–H bond and movement of hydrogen by hopping and/or tunneling [Fig. 1(c)], two separate dangling bonds [Fig. 1(d)], i.e., a normal dangling bond and a hydrogen-related dangling bond, are created under illumination. In the new model, the following processes are further taken into account: Hydrogen is dissociated from a Si–H bond located near a hydrogen-related dangling bond as a result of nonradiative recombination between an electron and a hole at the hydrogen-related dangling bond [Fig. 2(a)]. A dissociated hydrogen atom (metastable hydrogen atom) has a destiny in the following three ways. (1) Insertion process: It is inserted into a nearby weak Si–Si bond to form a

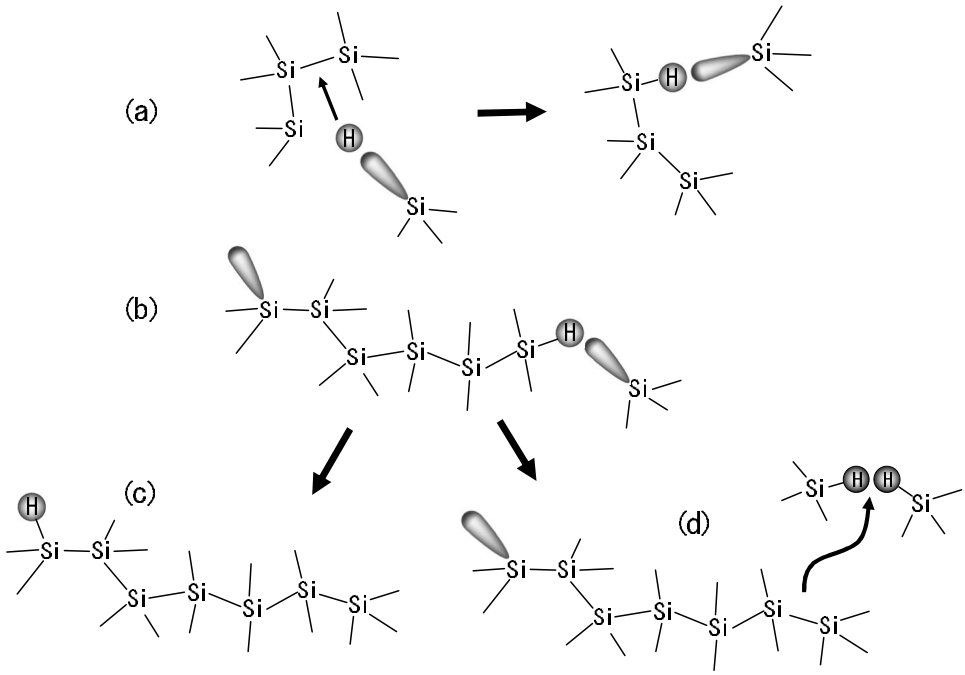

FIG. 2. (a) Insertion of a hydrogen atom into a nearby weak Si-Si bond following the formation of a hydrogen-related dangling bond. (b) Two separate dangling bonds and dissociation of a hydrogen atom from a hydrogen-related dangling bond. (c) Termination of a normal dangling bond by a dissociated hydrogen atom. (d) Termination of a hydrogen-related dangling bond by a dissociated hydrogen atom and formation of a hydrogen pair.

hydrogen-related dangling bond [Fig. 2(a)]. (2) Termination process: It terminates either a normal dangling bond [Fig. 2(c)] or a hydrogen-related dangling bond [Fig. 2(d)]. (3) Hydrogen-molecule-formation process: A dissociated hydrogen atom has a chance to form a hydrogen molecule by meeting together. In this new model, metastable hydrogen atoms dissociated from Si–H bonds located near hydrogen-related dangling bonds also play an essential role in light-induced defect creation in *a*-Si:H. Such a dissociation of hydrogen atoms was first suggested for thermal annealing processes of dangling bonds[33] and after then light-induced annealing processes of dangling bonds were recognized in which annihilation of light-induced dangling bonds is enhanced under illumination.[34] Direct evidence for light-induced annealing of dangling bonds has been observed for *a*-Si:H samples containing a large amount of hydrogen, in which, after illumination is turned on, the dangling bond ESR signal decays in intensity instead of its increase corresponding to the light-induced creation of dangling bonds.[34]

In the following, the light-induced defect creation is considered in terms of a rate-equation model, taking into account the processes mentioned above. Rate equations are given as follows:

$$dN_a/dt = C_d np(N_w/N_{w0}) - C_2 N_m N_a, \quad (1)$$

$$dN_b/dt = C_d np(N_w/N_{w0}) - C_1 npN_b + C_3 N_m N_{\mathrm{Si}} - C_4 N_m N_b, \quad (2)$$

$$dN_m/dt = C_1 npN_b - C_2 N_m N_a - C_3 N_m N_{\mathrm{Si}} - C_4 N_m N_b - C_5 N_m^2, \quad (3)$$

$$dN_w/dt = -C_d np(N_w/N_{w0}) + C_2 N_m N_a + C_4 N_m N_b, \quad (4)$$

where N_a, N_b, N_m, N_{Si}, N_w, N_{w0}, n, and p are densities of normal dangling bonds, hydrogen-related dangling bonds, metastable hydrogen atoms, Si–Si bonds, weak Si–Si bonds adjacent to a Si–H bond, N_w at $t=0$, free electrons, and free holes including band-tail electrons and holes, respectively, and C_d, C_1, C_2, C_3, C_4, and C_5 are reaction coefficients of the following processes. These processes are illustrated in Figs. 3(a) and 3(b): C_d the light-induced creation of two separate dangling bonds, C_1 the dissociation of a hydrogen atom from a Si–H bond located near a hydrogen-related dangling bond, C_2 the termination of a normal dangling bond by a metastable hydrogen atom, C_3 the insertion of a metastable hydrogen atom into a Si–Si bond, C_4 the termination of a hydrogen-related dangling bond by a metastable hydrogen atom, and C_5 the formation of a hydrogen molecule by two metastable hydrogen atoms, respectively. In Eq. (4), the density of weak Si–Si bonds decreases with the formation of dangling bonds and increases with the termination of dangling bonds by hydrogen atoms because a Si–Si bond adjacent to a Si–H bond is considered to become a weak bond. For high-quality *a*-Si:H, the C_3 term is neglected because the density of weak Si–Si bonds is relatively small compared to low-quality *a*-Si:H containing a large amount of hydrogen. In numerical calculations, the C_5 term is also neglected for simplicity.

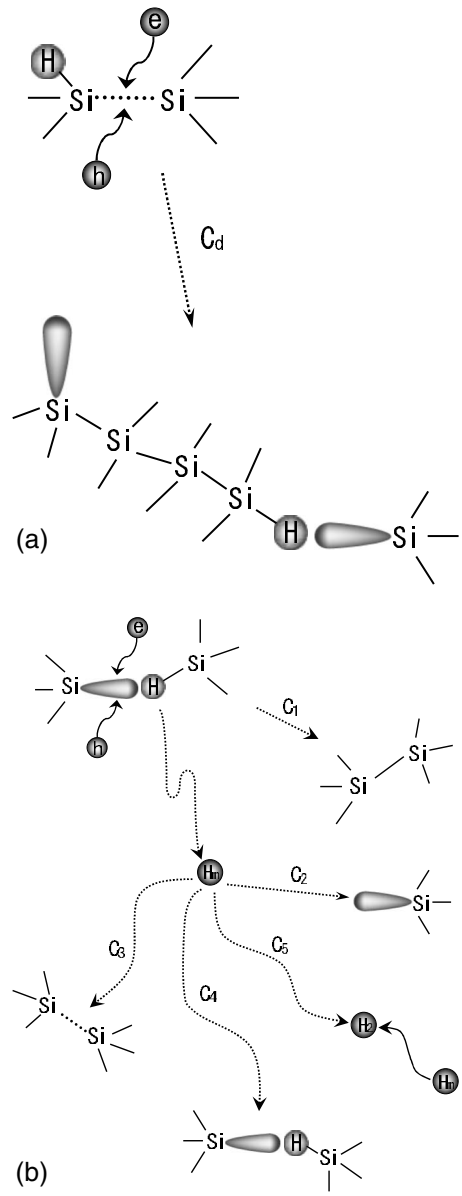

FIG. 3. Illustrations for reactions (a) C_d and (b) C_1, C_2, C_3, C_4, and C_5. See the text for definitions of these parameters.

In the following section, we consider the case of weak (continuous) illumination, so that we may neglect change in N_w with illumination, i.e., N_w is assumed to be equal to N_{w0} in Eqs. (1), (2), and (4). This is the case considered in previous publications.[18–20] The case of intense pulsed illumination has been considered, taking into account Eq. (4) in Refs. 21 and 22.

III. CALCULATION AND EXPERIMENT

A. Continuous illumination

1. Calculation

The carrier densities n and p are assumed to be determined by their steady-state values and by trapping of carriers (electrons) at neutral dangling bonds followed by rapid re-

combination with holes. They are proportional to G/N_d, where G and N_d are the generation rate of free carriers and the total density of neutral dangling bonds, respectively, because the trapping process at neutral dangling bonds of carriers in the conduction band and its tail states occurs faster than the kinetics of light-induced creation of dangling bonds. The steady-state values of n and p are approximately

$$n = p \cong G/(\alpha N_d), \tag{5}$$

where α is the trapping coefficient of free carriers by neutral dangling bonds. Then, in order to solve the rate equation numerically, the rate equations (1)–(3) are rewritten using normalized densities of N_a, N_b, and N_m to N_{d0} [$\equiv N_d(t=0)$], i.e., r, q, and s, respectively, as follows:

$$dr/dt = A/(r+q)^2 - A_2 sr, \tag{6}$$

$$dq/dt = A/(r+q)^2 - A_1 q/(r+q)^2 + A_3 s - A_4 sq, \tag{7}$$

$$ds/dt = A_1 q/(r+q)^2 - A_2 sr - A_3 s - A_4 sq - A_5 s^2, \tag{8}$$

$$r = N_a/N_{d0}, \tag{9}$$

$$q = N_b/N_{d0}, \tag{10}$$

$$s = N_m/N_{d0}, \tag{11}$$

$$N_d = N_a + N_b, \tag{12}$$

$$A = C_d G^2/\alpha^2 N_{d0}^3, \tag{13}$$

$$A_1 = C_1 G^2/\alpha^2 N_{d0}^2, \tag{14}$$

$$A_2 = C_2 N_{d0}, \tag{15}$$

$$A_3 = C_3 N_{\mathrm{Si}}, \tag{16}$$

$$A_4 = C_4 N_{d0}, \tag{17}$$

$$A_5 = C_5 N_{d0}. \tag{18}$$

In the following, we estimate the values of parameters except for A_5 in the rate equation for high-quality a-Si:H samples. First, we estimate the value of A, assuming $C_d = 2 \times 10^{-15}$ cm^3 s^{-1}, $\alpha = 1 \times 10^{-8}$ cm^3 s^{-1}, $N_d(t=0) \equiv N_{d0} = 1 \times 10^{16}$ cm^{-3}, and $G = 1 \times 10^{22}$ cm^{-3} s^{-1}. The value of C_d is obtained from the estimate by Vignoli *et al.*[35] The value of α has been estimated by Godet.[26] Using these values, we obtain $A = 2 \times 10^{-3}$ s^{-1} which represents the formation of a normal dangling bond and a hydrogen-related dangling bond. The value of A_1 is estimated by using the following equation given by Takeda *et al.*;[34]

$$A_1 = b_2, \tag{19}$$

$$b_2 = B_2 (G/N_{d0})^2, \tag{20}$$

where b_2 and B_2 are defined by Eqs. (2) and (10) in the paper of Takeda *et al.*,[34] respectively. The estimated values of b_2 by Takeda *et al.*[34] range between 0.25 and 11.5 h^{-1} for various samples of a-Si:H with dangling bond density of 10^{18} cm^{-3} and hydrogen content of 22–33 at. %, depending also on illumination intensity (0.7–1.5 W cm^{-2}). We take 1 h^{-1} ($=2.78 \times 10^{-4}$ s^{-1}) as the values of A_1 for $N_{d0} = 1 \times 10^{18}$ cm^{-3} and then we obtain A_1 of 2.78 s^{-1} for $N_{d0} = 1 \times 10^{16}$ cm^{-3} using Eq. (20). However, the value of b_2 is not available for high-quality samples. For these samples, we expect the value of A_1 to be much smaller than those for the low-quality samples mentioned above. We assume $A_1 = 3 \times 10^{-3}$ s^{-1}.

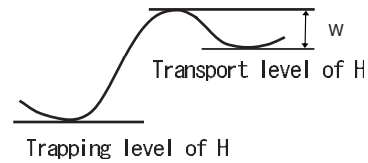

FIG. 4. Illustration for the trapping level and transport level of hydrogen.

For the estimate of A_2 related to C_2 which represents the termination of dangling bonds by a metastable hydrogen atom, we use two different values estimated by Godet[26] and Branz.[27] The value of C_2 of 3×10^{-20} cm^3 s^{-1} is obtained from Godet, in which C_2 corresponds to α_D in his paper. Then, we obtain $A_2 = 3 \times 10^{-4}$ s^{-1} using Eq. (15) and the value of $N_{d0} = 1 \times 10^{16}$ cm^{-3}. Branz gives the range of C_2 (k_{db} in his paper) to be 2×10^{-17} cm^3 s$^{-1} > C_2 > 1 \times 10^{-21}$ cm^3 s^{-1}. For $N_{d0} = 1 \times 10^{16}$ cm^{-3}, this gives 2×10^{-1} s$^{-1} > A_2 > 1 \times 10^{-5}$ s^{-1}. The value of $A_2 = 1 \times 10^{-3}$ s^{-1} is taken here.

A_3 is the reaction coefficient of the insertion of a metastable hydrogen atom into a Si-Si bond. For high-quality samples, there are few weak Si-Si bonds, so that the probability of a metastable hydrogen atom to find a nearby weak-bond site is very small. For simplicity, we assume $A_3 = 0$ for high-quality samples. However, for low-quality samples containing a large number of hydrogen, we assume $A_3 \neq 0$. For this case, the value of A_3 is estimated to be taken as the transition rate of hydrogen from a transport level into a trapping level in a Si-Si bond across the barrier height W (Fig. 4). Then, the value of A_3 is given by

$$A_3 = \nu_0 \exp(-W/k_B T), \tag{21}$$

where ν_0 and k_B are the attempt-escape frequency and the Boltzmann constant, respectively.

The value of W is estimated as follows: The binding energy of a trapped hydrogen at the BC site is about 1 eV.[36] Thus, W is expected to be smaller than 1 eV. A value of the transition energy has been theoretically obtained as 0.44 eV (Ref. 37) below the vacuum level. Since a more precise value of W is not available for a-Si:H, we take $W = 0.85$ and 0.95 eV as examples, and then, we obtain $A_3 = 5 \times 10^{-2}$ and 1×10^{-3} s^{-1}, respectively, at $T = 300$ K, assuming $\nu_0 = 1 \times 10^{13}$ s^{-1}. We use these values later for low-quality a-Si:H samples.

Concerning the value of A_4 related to C_4 which represents the termination of hydrogen-related dangling bonds by a metastable hydrogen atom, we take a tentative value in com-

parison with the value of A_2. Discussion on this point will be given later.

2. Comparison between calculation and experiment

In the following, we present calculated results on illumination time dependences of normal dangling bond density r, hydrogen-related dangling bond density q, total dangling bond density $r+q$, and metastable hydrogen density s, relative to the total density of dangling bonds before illumination for two cases which correspond to typical examples of experimental results taken by Stutzmann *et al.*[12] (case I) and Godet[26] (case II). Differences in the values of parameters between two samples will be discussed in the light of characterization of samples and their physical quantities. For case I, $r(t=0)=1$, $q(t=0)=0$, $C_d=2\times10^{-15}$ cm^3 s^{-1}, $C_1=3\times10^{-31}$ cm^6 s^{-1}, $C_2=1\times10^{-20}$ cm^3 s^{-1}, $C_3=0$, $C_4=1\times10^{-18}$ cm^3 s^{-1}, $C_5=0$, $\alpha=1\times10^{-8}$ cm^3 s^{-1}, and $N_d(t=0)=1\times10^{16}$ cm^{-3}. For case II, $r(t=0)=1$, $q(t=0)=0$, $C_d=4\times10^{-15}$ cm^3 s^{-1}, $C_1=3\times10^{-31}$ cm^6 s^{-1}, $C_2=1\times10^{-19}$ cm^3 s^{-1}, $C_3=C_4=C_5=0$, $\alpha=1\times10^{-8}$ cm^3 s^{-1}, and $N_d(t=0)=1\times10^{16}$ cm^{-3}. These values of the parameters are determined by fitting the experimental curves of $r+q$ vs illumination time to the calculated ones, taking into account the values of the parameters discussed in Sec. III A 1, as will be discussed below.

First, we present the calculated results of the light-induced dangling bond density as a function of illumination time in a high-quality sample used by Stutzmann *et al.*[12] and compare them with their experimental results which were obtained under illumination by a krypton-laser light at 1.9 eV and at 700, 400, 200, 100, and 50 mW/cm^2. The experimental points for 700 mW/cm^2 are first fitted to the calculated curve obtained by taking appropriate values of parameters shown above, as shown in Fig. 5(a). In order to estimate G, we used 1×10^{-4} cm^{-1} as the absorption coefficient for 1.9 eV in the sample of Stutzmann *et al.*, and then we obtain $G=2.3\times10^{22}$ cm^{-3} s^{-1}. The values of A and A_1–A_5 are obtained as follows: using Eqs. (13)–(18) for the values of C_d, C_1–C_5, α $(=1\times10^{-8}$ cm^3 s$^{-1})$, N_{d0} $(=1\times10^{16}$ cm$^{-3})$ and N_{Si}, $r(t=0)=r_0=1$, $q(t=0)=q_0=0$, $A=1.1\times10^{-2}$ s^{-1}, $A_1=1.6\times10^{-2}$ s^{-1} (a different value from Ref. 18 is used for A_1), $A_2=1\times10^{-4}$ s^{-1}, $A_3=0$, $A_4=1\times10^{-2}$ s^{-1}, $A_5=0$, and N_d $(t=0)=1\times10^{16}$ cm^{-3}. Then, we obtain calculated curves as functions of illumination time for other illumination intensities, i.e., 400, 200, 100, and 50 mW/cm^2, as shown in Figs. 5(b)–5(e), where the values of A and A_1 are obtained by Eqs. (13) and (14), using the same values of parameters as those for 700 mW/cm^2 except for G and the same values of A_2–A_5 are used as well. Although agreements between calculation and experiment are not good for 400, 200, 100, and 50 mW/cm^2, as seen in Figs. 5(b)–5(e), they seem satisfactory in a sense that the same values are used for the parameters except for G to obtain these calculated curves.

Next, we compare the experimental results obtained by Godet[26] with the calculated ones. Two different samples prepared at 250 °C by plasma-enhanced chemical vapor deposition (PECVD) from pure silane at a low power and a low pressure (standard PECVD a-Si:H) and by PECVD from silane diluted to helium at a high power (He-diluted PECVD a-Si:H) were used by Godet,[26] which were light soaked at 100 °C using a continuous xenon-arc lamp with the wavelengths below 570 nm ($G=1\times10^{22}$ cm^{-3} s^{-1}). Their experimental points are shown in Figs. 6(a) and 6(b) along with the calculated curves for each sample, respectively. The values of parameters used for the calculated curves are given as follows: For the standard PECVD a-Si:H [Fig. 6(a)], $r(t=0)=1$, $q(t=0)=0$, $A=4\times10^{-3}$ s^{-1}, $A_1=3\times10^{-3}$ s^{-1}, $A_2=1\times10^{-3}$ s^{-1}, $A_3=0$, $A_4=0$, $A_5=0$, and N_d $(t=0)=1\times10^{16}$ cm^{-3}. For the He-diluted PECVD a-Si:H [Fig. 6(b)], $r(t=0)=1$, $q(t=0)=0$, $A=7.28\times10^{-5}$ s^{-1}, $A_1=3.46\times10^{-4}$ s^{-1}, $A_2=1\times10^{-5}$ s^{-1}, $A_3=A_4=A_5=0$, and N_d $(t=0)=3.8\times10^{16}$ cm^{-3}. The fit of the calculated curve to the experimental points is excellent for the standard a-Si:H [Fig. 6(a)], while the calculated curve is not well fitted to the experimental points for the He-diluted a-Si:H [Fig. 6(b)]. Further, we attempted to fit the experimental points for the He-diluted a-Si:H in the long illumination time using $A_4=1\times10^{-5}$ s^{-1} and the same values of other parameters as above. The result is more satisfactory than that shown in Fig. 6(b), as shown in Fig. 6(c).

For the standard PECVD a-Si:H, the above values of A and A_1–A_5 correspond to case II mentioned above, i.e., $C_d=4\times10^{-15}$ cm^3 s^{-1}, $C_1=3\times10^{-31}$ cm^6 s^{-1}, $C_2=1\times10^{-19}$ cm^{-3} s^{-1}, and $C_3=C_4=C_5=0$, respectively, taking $\alpha=1\times10^{-8}$ cm^3 s^{-1} and $G=1\times10^{22}$ cm^{-3} s^{-1}. For the He-diluted PECVD a-Si:H, the above values of A and A_1–A_5 in Fig. 6(c) correspond to $C_d=4.39\times10^{-15}$ cm^3 s^{-1}, $C_1=5.31\times10^{-31}$ cm^6 s^{-1}, $C_2=C_4=2.63\times10^{-22}$ cm^{-3} s^{-1}, and $C_3=C_5=0$, taking $\alpha=1\times10^{-8}$ cm^3 s^{-1} and $G=1\times10^{22}$ cm^{-3} s^{-1}.

The He-diluted PECVD sample contains more dangling bonds and more hydrogen than the standard PECVD a-Si:H. This fact suggests that the He-diluted a-Si:H shows higher values of C_d and C_1 than the standard a-Si:H, being consistent with the experimental results. The hydrogen content in this sample is similar to that of the sample of Stutzmann *et al.*, so that it is plausible that $C_4\neq0$. Furthermore, we consider differences in the values of parameters A_2 and A_4 between the standard a-Si:H and the He-diluted a-Si:H. The typical features of two types of samples are quantities of bonded hydrogen content, structural factor R, and drift mobility at room temperature, i.e., 6.5 and 12.5 at. %, 0.06 and 0.4, and 1.7 and 0.3 cm^2 V^{-1} s^{-1}, respectively,[38] where R is the ratio of [2090]/([2090]+[2000]), in which [2090] and [2000] are the intensity of the stretching IR band centered at about 2090 cm^{-1}, attributed to IR absorption of SiH_2 and $(SiH_2)_n$, and that of the stretching IR band centered at about 2000 cm^{-1}, attributed to IR absorption of SiH, respectively. Furthermore, it has been suggested that the hydrogen diffusion is slow compared to that in the standard a-Si:H owing to the existence of nanovoids that has been evidenced from small-angle x-ray scattering.[39,40] The latter result is consistent with the difference in the value of parameter A_2 between two types of samples, namely, when the hydrogen diffusion is slow, this value becomes small. This is the case for the He-diluted a-Si:H.

We compare the values of parameters obtained for two cases of Stutzmann *et al.*[12] and Godet[26] (standard a-Si:H). A

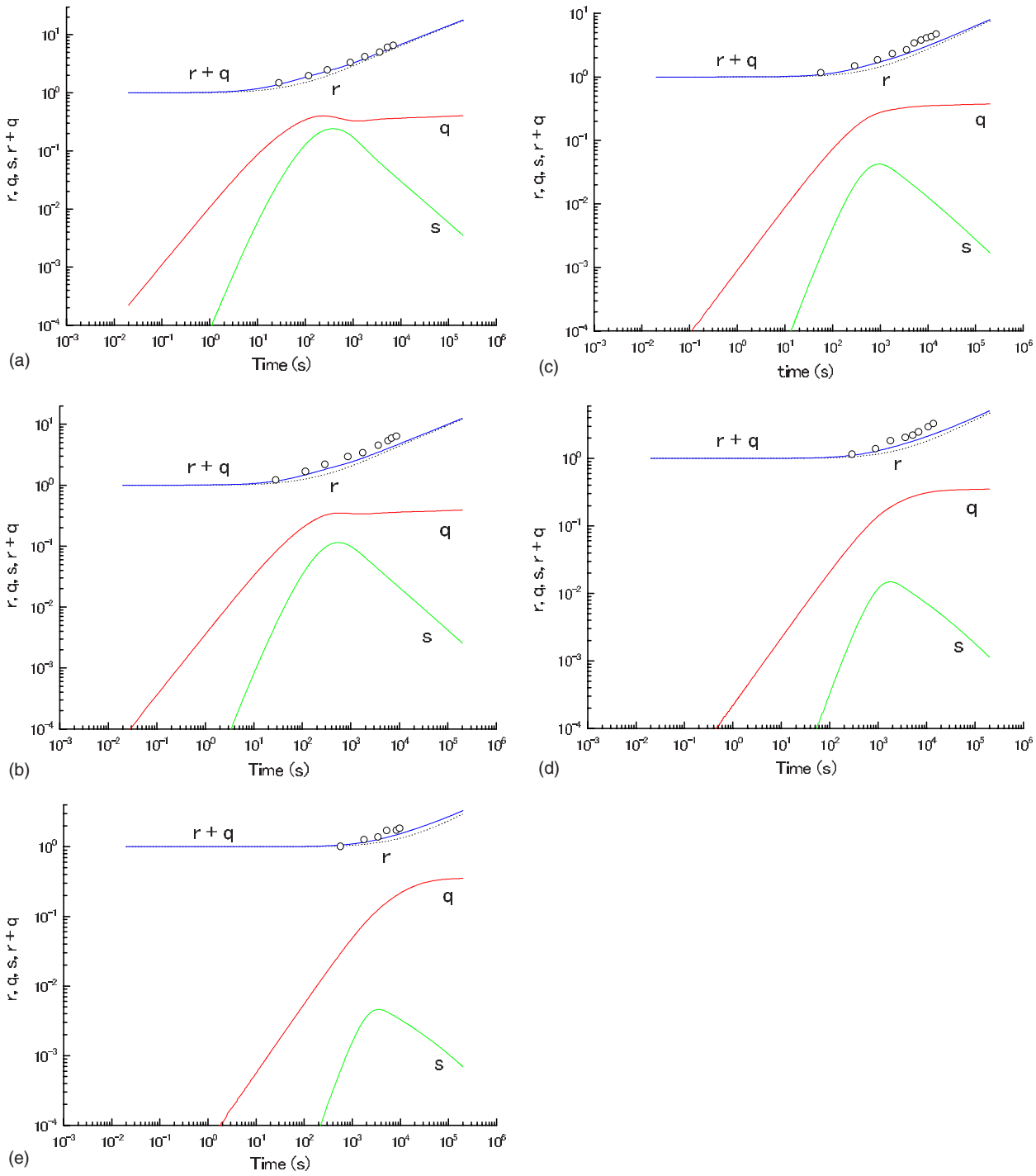

FIG. 5. (Color online) Calculated densities of total dangling bonds, $r+q$, normal dangling bonds, r, hydrogen-related dangling bonds, q, and metastable hydrogen atoms, s, relative to $N_{d0}=1\times10^{16}$ cm^{-3} as functions of illumination time for the case of Stutzmann *et al.* (Ref. 12) as well as their experimental points for illumination intensities of (a) 700 mW cm^{-2}, (b) 400 mW cm^{-2}, (c) 200 mW cm^{-2}, (d) 100 mW cm^{-2}, and (e) 50 mW cm^{-2}. The calculated curves are shown by solid lines except for r shown by a dotted line. For the values of parameters used in the calculation, see the text.

significant difference between the two cases is the values of A_4, which are 0.01 s^{-1} and 0 for Stutzmann *et al.*[12] and Godet,[26] respectively. This arises from a difference in preparation conditions, although both samples are prepared at nearly the same temperatures, i.e., 230 and 250 °C by PECVD, respectively, using pure silane. Stutzmann *et al.* used normal condition for rf power and gas pressure at 230 °C, but Godet used low power and low pressure. The hydrogen content is >10 and 6.5 at. % for both, respectively. Since the dangling bond density is the same as 1×10^{16} cm^{-3}, the difference in A_4 comes from the value of C_4 that is the termination coefficient of a hydrogen atom to a

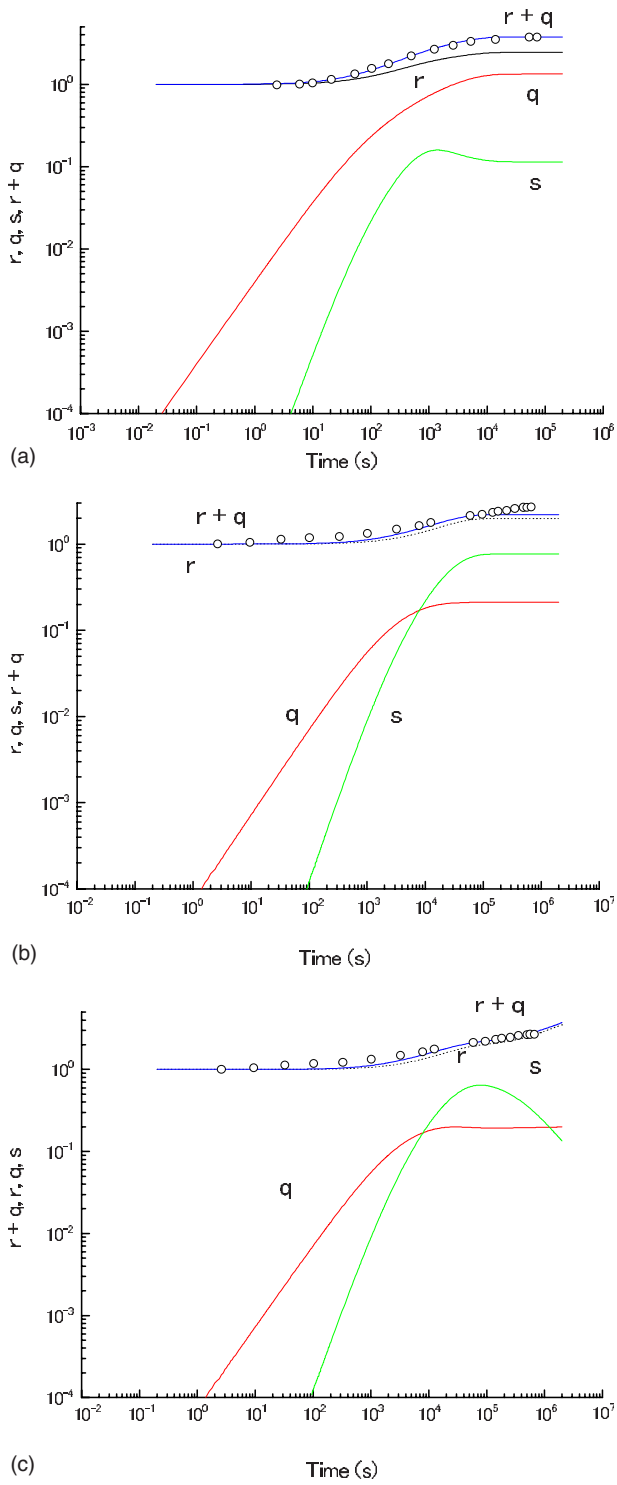

FIG. 6. (Color online) Calculated densities of total dangling bonds, $r+q$, normal dangling bonds, r, hydrogen-related dangling bonds, q, and metastable hydrogen atoms, s, relative to $N_{d0}=1\times10^{16}$ cm^{-3} as functions of illumination time for the case of Godet (Ref. 26) as well as his experimental points for (a) standard PECVD a-Si:H and [(b) and (c)] He-diluted PECVD a-Si:H. The calculated curves are shown by solid lines except for r shown by a dotted line. For the values of parameters used in the calculation, see the text.

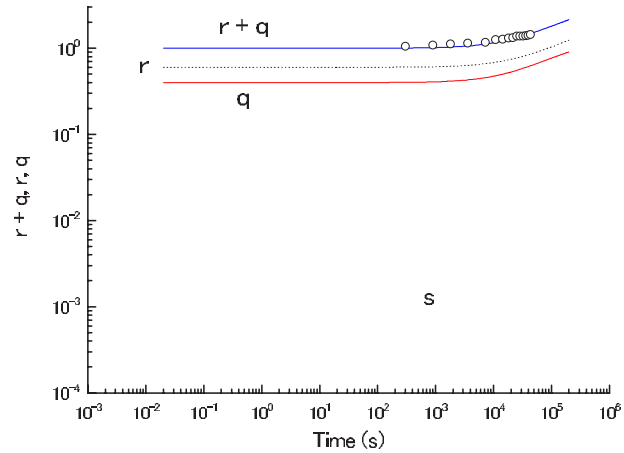

FIG. 7. (Color online) Calculated densities of total dangling bonds, $r+q$, normal dangling bonds, r, hydrogen-related dangling bonds, q, and metastable hydrogen atoms, s, relative to $N_{d0}=3.4\times10^{18}$ cm^{-3} as functions of illumination time for the case of a PECVD a-Si:H No. 1538 (Ref. 34) as well as the experimental points. The calculated curves are shown by solid lines except for r shown by a dotted line. For the values of parameters used in the calculation, see the text.

hydrogen-related dangling bond. It seems to us that, judging from the hydrogen content and other structural information, the sample of Stutzmann *et al.* has a more flexible network than Godet's sample. The value of C_4 seems to be related to local distortion around the hydrogen-related dangling bond, so that the above difference in the value of C_4 seems reasonable to us. On the other hand, the value of A_2 (C_2) is opposite to that of A_4 (C_4), i.e., the value of A_2 is 0.0001 s^{-1} for Stutzmann *et al.* and 0.001 s^{-1} for Godet. This quantitative difference should be accounted for in terms of a quantitative calculation of the termination coefficient of a hydrogen atom to a normal dangling bond. This is beyond the scope of this paper, so it is left behind as a future problem.

In the following, we present the calculated result on a PECVD sample No. 1538 prepared at 100 °C, using pure silane.[34] This sample contains a large amount of hydrogen with [H]>32 at. %. A similar sample exhibits a local electron-nuclear double resonance (ENDOR) signal due to hyperfine interaction of the dangling bond electron with a nearby hydrogen.[41–44] Further, light soaking results in the creation of almost equal number of two types of dangling bonds, i.e., normal dangling bonds and hydrogen-related dangling bonds.[41,45] The deconvolution of the ESR spectrum in the dark for a-Si:H No. 1538 is also consistent with this result,[46] that is, two types of dangling bonds almost equally exist in the dark. An example of the fit of the dangling bond density normalized to that in the dark ($N_{d0}=3.4\times10^{18}$ cm^{-3}) is shown in Fig. 7, where experimental points[34] are shown by open circles and the values of parameters used for the fit are $A=1\times10^{-5}$ s^{-1}, $A_1=1\times10^{-4}$ s^{-1}, $A_2=1\times10^{-3}$ s^{-1}, $A_3=5\times10^{-2}$ s^{-1}, $A_4=1\times10^{-3}$ s^{-1}, and $A_5=0$. The values of r_0 and q_0 before illumination by a xenon-arc lamp at 0.7 W/cm^2 are taken to be 0.6 and 0.4, respectively. From the values of A and A_1, we obtain $C_d=3.9\times10^{-10}$ cm^3 s^{-1} and $C_1=1.2\times10^{-27}$ cm^6 s^{-1}, respectively,

taking $\alpha=1\times10^{-8}$ cm^3 s^{-1}, $G=1\times10^{22}$ cm^{-3} s^{-1}, and $N_{d0}=3.4\times10^{18}$ cm^{-3}. The values of C_d and C_1 are reasonable as those for low-quality samples such as Sample No. 1538, as discussed in Sec. III A 1. For low-quality samples, C_3 has a finite value, i.e., A_3 is expected to be finite, as mentioned in Sec. II, where two values of A_3 are estimated to be 5×10^{-2} and 1×10^{-3} s^{-1}. Here, we take $A_3=5\times10^{-2}$ s^{-1}. The overall fit is good, as seen in Fig. 7. The values of the parameters used for the fit are reasonable as those for low-quality samples, as discussed above and in Sec. III A 1.

In the following, we discuss the ratio of r to q for the above-considered cases. For high-quality a-Si:H samples, the ratio of r to q is equal to or more than 5 for the case of Stutzmann *et al.* (case I) and 2 for Godet's case (case II), depending on illumination time. In the case of Stutzmann *et al.*, the above ratio of r to q (=5) can be seen at $t\cong500$ s in Fig. 5(b). In the Godet case, the above ratio of r to q can be seen in the saturated dangling bond density [Fig. 6(a)]. In the above case, all of the dangling bonds before illumination, i.e., in the dark, are assumed to be normal dangling bonds.

The ESR signal is usually given by a derivative of the ESR line, so that if the peak-to-peak separation gets twice, then the peak intensity of the derivative curve becomes four times smaller than before even for the same integrated intensity as before. The peak-to-peak separation of the ESR signal due to hydrogen-related dangling bonds is about twice larger than that due to normal dangling bonds[45] because the hyperfine dipolar interaction with hydrogen nucleus gives rise to the line broadening associated with the hyperfine doublet. These facts indicate that the peak intensity of the ESR signal due to hydrogen-related dangling bonds becomes 8 times smaller than that due to normal dangling bonds for the Godet case. For the case of Stutzmann *et al.*, the peak intensity of the ESR signal due to hydrogen-related dangling bonds becomes 20 times smaller than that due to normal dangling bonds. Thus, even if the hydrogen-related dangling bonds are created after prolonged illumination, change in the line shape with the ESR signal due to hydrogen-related dangling bonds is subtle. This is the case for high-quality a-Si:H samples. This is the reason why the line shape has been reported not to change after prolonged illumination except for the case of intense pulsed illumination. Very recently, Astakhov *et al.*[47] observed a broadening of the line shape, particularly in the high magnetic field side of the ESR line after 2 MeV electron irradiation at 100 K in a-Si:H. This broadening can be accounted for by superposition of an additional line coming from hydrogen-related dangling bonds as a result of the deconvolution of the ESR line into two components due to normal dangling bonds and hydrogen-related dangling bonds.

For low-quality a-Si:H samples, the observation of hydrogen-related dangling bonds has been done from ESR and ENDOR measurements in a-Si:H[41–46] and a-Si:D.[44,48]

Further, it is interesting to note that a similar defect to the hydrogen-related dangling bond, i.e., so called vacancy-hydrogen complex, has been observed by Nielsen *et al.*[49] in H-implanted crystalline silicon (c-Si). The hyperfine interaction constants with a hydrogen nucleus estimated by them are similar to those deduced from ENDOR measurements on a-Si:H.[41,44]

3. Thermal annealing mechanism

In the following, we consider the thermal annealing mechanism for light-induced dangling bonds in terms of the model for light-induced defect creation in a-Si:H presented in this paper. When a hydrogen atom is thermally dissociated from a Si-H bond located near a hydrogen-related dangling bond, it moves to a normal dangling bond site and then it terminates a normal dangling bond. As a result, both dangling bonds are annihilated. For high-quality a-Si:H samples, however, normal dangling bonds are normally photocreated much more than hydrogen-related dangling bonds. Therefore, we must consider other annealing processes. The following two processes are considered: First, we consider hydrogen dissociation from two closely located Si-H bonds created from the termination of a hydrogen atom to a hydrogen-related dangling bond under illumination. The dissociation energy of a hydrogen atom from a Si-H bond within a closely located Si-H bond pair has not been estimated, but it seems to be smaller than that of an isolated Si-H bond.[23,36] Second, we consider hydrogen dissociation from a hydrogen molecule. Hydrogen atoms are created under illumination whose density strongly depends on illumination time, as shown in Figs. 5(a) and 6(a). We have neglected the formation process of hydrogen molecules from hydrogen atoms in the calculation to be compared with experimental results. However, hydrogen atoms are encountered to form hydrogen molecules under illumination. Recent NMR measurements suggest that there are present hydrogen molecules at 10% (Ref. 50) and 2–40% (Ref. 51) of total hydrogen content in PECVD samples. The dissociation energy of hydrogen molecules in crystalline silicon has been calculated by Van de Walle and Tuttle[52] to be 1.74 eV for dissociation to two hydrogen atoms and 1.34 eV for dissociation to positively and negatively charged hydrogen ions (a hydrogen cation and a hydrogen anion). These values of dissociation energy are higher than the activation energy of thermal annealing, i.e., ~1 eV (see, e.g., Ref. 5), but they seem reasonable to us if distribution of activation energy extending toward higher than 1 eV is taken into account. For the first annealing process mentioned above, this consideration is also applied. As the third annealing process, the reconstruction of silicon network may be taken into account, as was pointed by Zukotynski *et al.*[53] Their annealing measurements on photoluminescence spectra in a-Si:H containing hydrogen and tritium also indicate that the dissociation of hydrogen from monohydride (Si-H) clusters and its termination with dangling bonds (the formation of Si-H bonds) are involved in the annealing process as well as the reconstruction of silicon network. This result also suggests that the reversible equilibrium reaction between dangling bonds +hydrogen and Si-H bonds takes place in the amorphous network of a-Si:H.

B. Saturated light-induced dangling bond density

It has been reported that saturation of the light-induced dangling bond density occurs with increasing the illumination time for some of high-quality a-Si:H samples.[26,54–57] In the present model, this is the case for $C_4=0$ in which hydro-

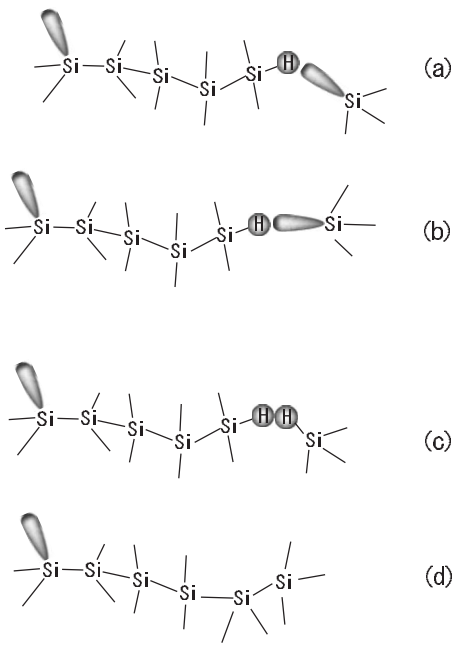

FIG. 8. Atomic configurations of two pairs of a normal dangling bond and a hydrogen-related dangling bond: [(a) and (b)] before dissociation of hydrogen and [(c) and (d)] after termination of a hydrogen-related dangling bond by a dissociated hydrogen.

gen atoms dissociated from hydrogen-related dangling bonds terminate normal dangling bonds with some probability and otherwise they remain as free hydrogen atoms becoming eventually hydrogen molecules as a result of their collision. After dissociation of hydrogen atoms from hydrogen-related dangling bonds, the dangling bonds are annihilated, and if they terminate normal dangling bonds, these two separate dangling bonds are annihilated, so that saturation of dangling bonds occurs with increasing illumination time and the dangling bond density reaches the steady-state value. If $C_4 \neq 0$, two normal dangling bonds are left behind when dissociated hydrogen atoms terminate nearby hydrogen-related dangling bonds, as illustrated in Fig. 8.

The saturated light-induced dangling bond density can be obtained as follows: The right-hand sides of Eqs. (1)–(3) are set equal to zero. The following relationship deduced from considerations that normal dangling bonds are equally photocreated with hydrogen-related dangling bonds and that a metastable hydrogen atom is photocreated from a hydrogen-related dangling bond is used:

$$\Delta N_a = \Delta N_b + \Delta N_m, \tag{22}$$

where Δ means "photocreated." Equation (4) is neglected because we deal with the situation that weak bonds exist enough to create dangling bonds by prolonged illumination corresponding to the continuous illumination. Further, we treat the case of high-quality a-Si:H samples, so that we have $C_3=0$. For simplicity, we assume $C_5=0$, as was mentioned before.

In the following, we treat two cases, i.e., (1) monomolecular recombination case [Eq. (5) is held] and (2) bimolecular recombination case,

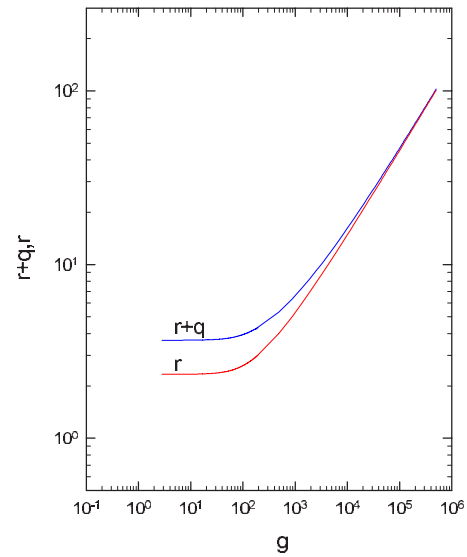

FIG. 9. (Color online) Calculated saturated densities of total dangling bonds, $r+q$, and normal dangling bonds, r, relative to $N_{d0}=1\times10^{16}$ cm^{-3} as a function of generation rate relative to 10^{20} cm^{-3} s^{-1}, g, for the monomolecular recombination case.

$$n = p \cong (G/\beta)^{1/2}, \tag{23}$$

where β is the recombination coefficient of free electrons (or tail electrons) and free holes (or tail holes). The bimolecular recombination case occurs under intense illumination.

For the monomolecular recombination case, we obtain the following relationship of the saturated densities of light-induced normal dangling bonds and hydrogen-related dangling bonds ΔN_{as} and ΔN_{bs}:

$$\Delta N_{as} = (C_d/2C_1)\{1 + [1 + 4(C_1^2G^2/\alpha^2\Delta N_{ss}^2 C_d C_2)]^{1/2}\}, \tag{24}$$

$$\Delta N_{bs} = C_d/C_1, \tag{25}$$

where $\Delta N_{ss}=\Delta N_{as}+\Delta N_{bs}$ and we assume $N_a(t=0)=N_{d0}$, $N_b(t=0)=0$, and $N_m(t=0)=0$, so that we have $\Delta N_{as}=N_{as}-N_{d0}$, $\Delta N_{bs}=N_{bs}$, and $\Delta N_m=N_m$. Reminding us that the right-hand side of Eq. (24) includes ΔN_{ss} $(=\Delta N_{as}+\Delta N_{bs})$, Eq. (24) is solved numerically as a function of G for a case that $C_d=4\times10^{-15}$ cm^3 s^{-1}, $C_1=3\times10^{-31}$ cm^6 s^{-1}, $C_2=1\times10^{-19}$ cm^3 s^{-1}, $C_3=C_4=C_5=0$, and $\alpha=10^{-8}$ cm^3 s^{-1}. The result is shown in Fig. 9, where r $(=N_{as}/N_{d0})$ and $r+q$ $(=N_{ss}/N_{d0})$ are plotted against G relative to 10^{20} cm^{-3} s^{-1}, g, and N_{d0} is 1×10^{16} cm^{-3}. The value of C_d corresponds to that for high-quality a-Si:H samples. The above values of parameters are the same as those used previously for the case of Godet. From Eq. (25), we note that ΔN_{bs} is independent of G.

The approximate solution of N_{ss} is obtained for two extreme cases: For weak illumination, N_{as} is approximately by

$$N_{as} \cong (C_d/C_1) + N_{d0}. \tag{26}$$

Then, we obtain

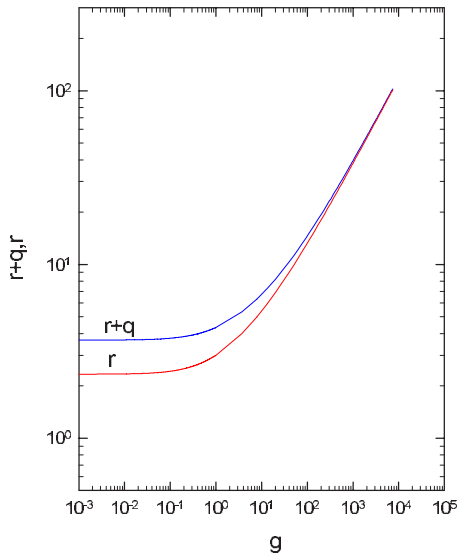

FIG. 10. (Color online) Calculated saturated densities of total dangling bonds, $r+q$, and normal dangling bonds, r, relative to $N_{d0}=1\times10^{16}$ cm^{-3} as a function of generation rate relative to 10^{20} cm^{-3} s^{-1}, g, for the bimolecular recombination case.

$$N_{ss} \cong 2(C_d/C_1) + N_{d0}. \tag{27}$$

Equations (26) and (27) show that N_{as} and N_{ss} tend to a constant value, i.e., 2.33×10^{16} and 3.67×10^{16} cm^{-3}, respectively, with decreasing the carrier generation rate, as seen in Fig. 9, where dangling bond densities relative to 10^{16} cm^{-3} are shown as functions of carrier generation rate relative to 10^{20} cm^{-3} s^{-1} and the initial value of N_d at $t=0$($\equiv N_{d0}$) is 1×10^{16} cm^{-3}. For strong illumination, N_{as} is approximately by

$$N_{as} \cong (C_d/C_2)^{1/4}(G/\alpha)^{1/2} + N_{d0}. \tag{28}$$

Equation (28) shows that N_{as} has a square-root dependence on G for large G, as seen in Fig. 9.

As seen in Fig. 9, N_{ss} tends to reach a certain value with decreasing G. This means that even if illumination intensity is very low, dangling bonds with a certain density may be created by prolonged illumination. The kinetics of light-induced creation of dangling bonds is considered in the next section, where it is shown that it takes a long time for dangling bonds to reach a saturated density, N_{ss}, when illumination intensity is very low. This is quite reasonable.

For the bimolecular recombination case, we obtain

$$N_{as} = (C_d/2C_1)\{1 + [1 + 4(C_1^2 G/\beta C_d C_2)]^{1/2}\} + N_{d0}, \tag{29}$$

$$N_{bs} = (C_d/C_1). \tag{30}$$

N_{as} is obtained numerically as a function of G for a case that $C_d=4\times10^{-15}$ cm^3 s^{-1}, $C_1=3\times10^{-31}$ cm^6 s^{-1}, $C_2=1\times10^{-19}$ cm^3 s^{-1}, $C_3=C_4=C_5=0$, and $\beta=3\times10^{-8}$ cm^3 s^{-1}, where we use a relation of $\beta=3\alpha$ found by Stutzmann *et al.*[58] The result is shown in Fig. 10, which is almost similar to that for the monomolecular recombination case. As shown in Figs. 9 and 10, the light-induced dangling bond density exceeds 10^{18} cm^{-3} for intense illumination such as pulsed illumination, being consistent with the observation by Stutzmann *et al.*[58] We treat more exactly the case of pulsed intense illumination in which the density of weak bonds is also taken into account.[21,22] From Eq. (30), we note that N_{bs} is independent of G similarly to the monomolecular recombination.

In the following, we consider the experimental results on the illumination-intensity dependence of the saturated light-induced dangling bond density cited from the literature. For weak illumination, the value of N_{ss} is almost independent of the carrier generation rate, i.e., illumination intensity. Two data are cited from the literatures, one of them[55,56] shows $N_{ss}\propto G^{\gamma}$ with $\gamma=0.24$ in the range of 4×10^{21}–3×10^{22} cm^{-3} s^{-1} and the other[57] with $\gamma=0.41$ in the range of 5.2×10^{22}–9.4×10^{22} cm^{-3} s^{-1}. Both data have been taken for high-quality a-Si:H samples. For these generation-rate ranges, the monomolecular recombination case is taken, so that we compare those results with the calculated slope γ of $\log N_s$ vs G, i.e., $\gamma=0.46$ between 5×10^{22} and 1×10^{23} cm^{-3} s^{-1} and a smaller slope for less than 5×10^{22} cm^{-3} s^{-1} from Fig. 8. These values are consistent with the observations mentioned above.

Concerning the hydrogen-content dependence of the saturated light-induced dangling bond density, we cite a report by Godet *et al.*[59] that the value of N_{ss} is proportional to dilute phase Si-H bond density. For the carrier generation rate below 10^{19} cm^{-3} s^{-1}, the value of N_{ss} is almost determined by Eq. (27), i.e., $2C_d/C_1$. Vignoli *et al.*[35] reported that the value of C_d is linearly correlated with the structural factor R indicating the clustered hydrogen content percentage relative to total hydrogen content. The value of C_1 seems to us to increase with increasing hydrogen content, but this hydrogen-content dependence may be weaker than that of C_d, particularly in the high-quality samples. Taking into account that dilute phase Si-H bond density is obviously correlated with densities of Si-H_2 bonds and clustered Si-H bonds, the observed result on N_{ss} vs Si-H bond density is consistent with the above prediction.

The illumination-temperature dependence of N_{ss} is also discussed from Eqs. (27) or (28). According to Wu *et al.*,[57] the value of N_{ss} decreases with increasing illumination temperature between 21 and 120 °C with an activation energy of 0.046 eV. According to Isomura *et al.*,[55,56] it decreases slightly from 25 to 100 °C and then decreases up to 130 °C with an activation energy of 0.14 eV. In these temperature ranges, the value of C_d has a weak temperature dependence, namely, it increases with increasing illumination temperature. On the other hand, the value of C_1 should also be activated, i.e., it increases with increasing illumination temperature. The activation energy of C_1 in the dark corresponds to that for thermal annealing of dangling bonds, i.e., 1 eV, but under illumination, it decreases as a result of the recombination-enhanced reaction associated with nonradiative recombination between an electron and a hole at a hydrogen-related dangling bond. The activation energy of illumination-temperature dependence of N_{ss} is determined by the competition between the activation energies of C_d and C_1. At present, however, a quantitative consideration on the activation energy of C_1 is beyond the scope of this paper, but

the values of 0.046 and 0.14 eV estimated by the above two groups suggest that C_1 has a stronger temperature dependence than C_d. The difference between the above two values seems to arise from those in samples and illumination intensities as well as C_d, depending on hydrogen content, etc.

In summary, a model presented here accounts for the observation that the saturated light-induced dangling bond density exceeds 10^{18} cm^{-3} under intense illumination. The dependences of saturated light-induced dangling bond density on illumination intensity, illumination temperature, and hydrogen content are also understood semiquantitatively or qualitatively in terms of the present model.

C. Stretched exponential function

The illumination-time dependence of light-induced dangling bond density, ΔN_{ss}, in a-Si:H has been fitted to a stretched exponential function as follows:[60–65]

$$N_d(t) = N_{ss} - [N_{ss} - N_d(0)]\exp[-(t/\tau)^{\beta}], \qquad (31)$$

where N_{ss}, β, and τ are the saturated dangling bond density (steady-state dangling bond density), a dispersion parameter, and a characteristic time, respectively. The stretched exponential function is usually derived from dispersive relaxation phenomena, e.g., the relaxation process associated with dispersive motion of hydrogen.[66] Our model shown in Sec. II involves several complex processes, in some of which dispersive motion of hydrogen plays an important role.[67] Thus, it is interesting how the calculated curve of N_d vs t is fitted to the stretched exponential function and to estimate the values of β and τ for various values of N_{ss}. The calculation was performed using $N_d(0)=1\times10^{16}$ cm^{-3} and the same values of parameters C_d, C_1, C_2, C_3, C_4, and C_5 as those for case II (Godet) in Sec. III A 2, except for C_2 in the case of $G=5\times10^{18}$ cm^{-3} s^{-1}, i.e., $C_2=1\times10^{-21}$ cm^3 s^{-1}. The obtained values of N_{ss}, β, and τ are given as follows: (1) $N_{ss}=3.67\times10^{16}$ cm^{-3}, $\beta=0.625$, and $\tau=5.58\times10^{15}$ s, (2) $N_{ss}=3.78\times10^{16}$ cm^{-3}, $\beta=0.632$, and $\tau=1.34\times10^{3}$ s, (3) $N_{ss}=3.67\times10^{16}$ cm^{-3}, $\beta=0.618$, and $\tau=5.02\times10^{4}$ s, (4) $N_{ss}=5.12\times10^{16}$ cm^{-3}, $\beta=0.631$, and $\tau=7.36\times10$ s, (5) $N_{ss}=9.88\times10^{16}$ cm^{-3}, $\beta=0.538$, and $\tau=1.55\times10$ s, and (6) $N_{ss}=2.21\times10^{17}$ cm^{-3}, $\beta=0.494$, and $\tau=4.92$ s, in which three examples of the fit of the calculated curve to the stretched exponential function for cases (2), (4), and (5) are shown in Figs. 11 (curves c, b, and a, respectively). The obtained values of β and τ are plotted as functions of N_{ss} in Figs. 12(a) and 12(b), respectively. The relationship between N_{ss} and G is shown in Fig. 13. As seen in the figure, N_{ss} for the weak G limit is 3.67×10^{16} cm^{-3}, which corresponds to case II (Godet) in Sec. III A 2. For all curves, the fit of the stretched exponential function to the calculated curves is good, except for the short-time tail region.

In the following, we discuss the β vs N_{ss} curve and the τ vs N_{ss} curve shown in Figs. 12(a) and 12(b), respectively. In these figures, the values of β and τ obtained by Godet[25] are also shown, where Godet's results[25] are calculated ones, except for one point for $N_{ss}=3.75\times10^{16}$ cm^{-3} for which the experimental N_d vs t curve is fitted to the stretched exponential function, as shown below. Godet presented a model for light-induced defect creation in a-Si:H that metastable hydrogen atoms are created from doubly hydrogenated (Si-HHSi) configurations as a result of recombination of electron-hole pairs under illumination and then they are trapped either at broken bonds or at Si-H bonds, corresponding to light-induced annealing and light-induced defect creation reactions, respectively. He considered his experimental result in terms of this model, i.e., metastable hydrogen trapping model and obtained the results of $\beta=0.52$, $\tau=1.5\times10^{3}$ s, and $N_{ss}=3.75\times10^{16}$ cm^{-3}. For this sample, our result of the fit is $\beta=0.63$, $\tau=1.3\times10^{3}$ s, and $N_{ss}=3.78\times10^{16}$ cm^{-3}. These values are almost in agreement with those obtained by Godet.[25] However, as shown in Figs. 12(a) and 12(b), there are some disagreements between these two models, particularly, the N_{ss} dependence of τ is completely opposite and there are great disagreements for high N_{ss}.

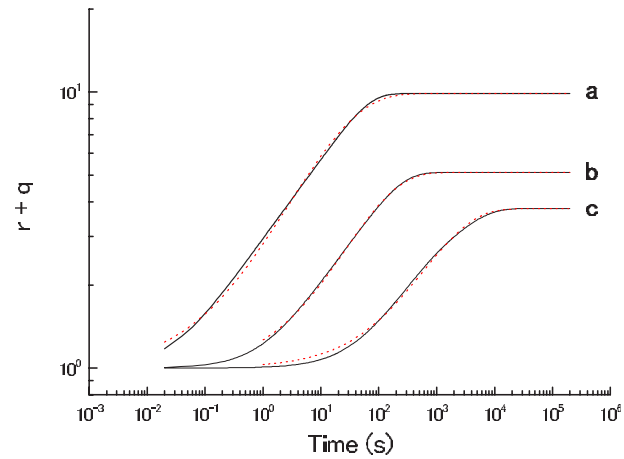

FIG. 11. (Color online) Fitting of calculated curves of $r+q$ vs illumination time (solid lines) by a stretched exponential function given by Eq. (31) (dotted line). Curves a, b, and c correspond to different illumination intensities, i.e., different generation rates as well as different values of parameters, i.e., cases (5), (4), and (2) (see the text for details).

The N_{ss} dependences of β and τ obtained from our model are reasonable, explained as follows: The increase in N_{ss} corresponds to the increase in the generation rate of electron-hole pairs. For high N_{ss}, we obtain small β and short τ. The value of β mainly determines the growing curve in the initial stage, i.e., when β is small, N_d initially grows up rapidly, while τ determines the characteristic of the growing curve in the long term, i.e., when τ is short, N_d grows up rapidly in the long term. Small β means that the distribution function of the inverse of lifetime of light-induced dangling bonds deduced from the Fourier transform of $N_d(t)$ in Eq. (31) is broadened (see Fig. 11.14 in Ref. 5). The value of τ corresponds to a time how the balance between light-induced defect creation and light-induced defect annealing goes on, so that it is related to (1) the creation of two separate dangling bonds, (2) the dissociation of hydrogen atoms from hydrogen-related dangling bonds, and (3) the termination of hydrogen atoms to normal dangling bonds. Items (1) and (3) are also related to the movement of hydrogen atoms when they separate two dangling bonds with their movement and when they terminate normal dangling bonds. Under intense

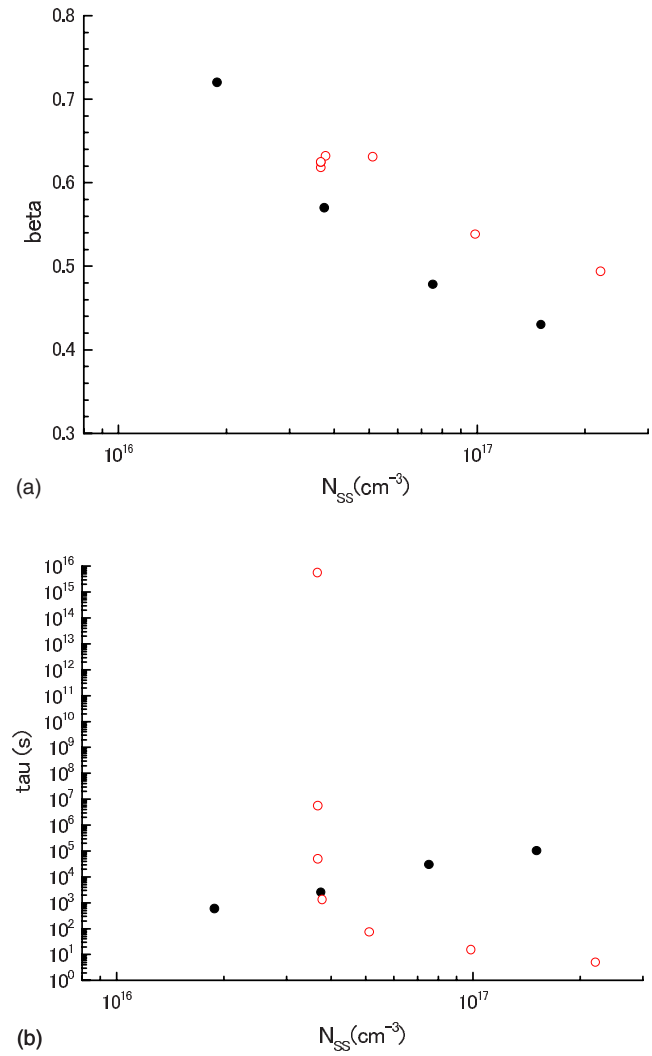

FIG. 12. (Color online) Calculated results of (a) β vs N_{ss} (saturated dangling bond density) and (b) τ vs N_{ss} by Godet (Ref. 25) (closed circles) and by the present work (open circles). See the text for details.

illumination, these reactions occur at many sites, namely, many hydrogen-related dangling bonds are created during illumination and many nearby hydrogen atoms are dissociated, so that the lifetime of light-induced dangling bonds distributes over a wide range from a short lifetime to a long lifetime. Then, τ becomes short compared to the case of weak illumination. On the other hand, as N_{ss} decreases under weak illumination, β tends to unity. This means a sharp distribution of the lifetime. When $\beta=1$, the stretched exponential function becomes a single exponential function with a well-defined characteristic time τ.

On the other hand, the Godet model[25] predicts a different tendency for τ against N_{ss} from our model, i.e., τ decreases with decreasing N_{ss}, as shown in Fig. 12(b). From the Godet model,[25] the metastable hydrogen atoms are generated directly by illumination from doubly hydrogenated (SiHHSi) sites, while in our model they are generated from hydrogen-related dangling bonds, i.e., their indirect generation by illumination. Thus, they easily terminate dangling bonds in the

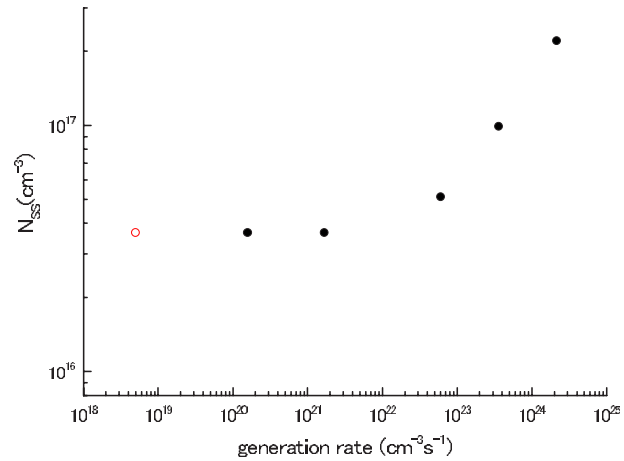

FIG. 13. (Color online) Calculated results of (a) N_{ss} vs generation rate using the following values of parameters: (closed circles) $C_d=4\times10^{-15}$ cm^3 s^{-1}, $C_1=3\times10^{-31}$ cm^6 s^{-1}, $C_2=1\times10^{-19}$ cm^3 s^{-1}, and $C_3=C_4=C_5=0$; (open circle) $C_d=4\times10^{-15}$ cm^3 s^{-1}, $C_1=3\times10^{-31}$ cm^6 s^{-1}, $C_2=1\times10^{-21}$ cm^3 s^{-1}, and $C_3=C_4=C_5=0$. See the text for details.

Godet model[25] in comparison with our model. In the Godet model, this causes the enhancement of the termination of light-induced dangling bonds by metastable hydrogen atoms, so that the growing rate of light-induced dangling bonds becomes slow, i.e., τ becomes long.

In comparison with the stretched exponential function, the case of Stutzmann *et al.*[12] being fitted to a power-law function is considered as follows. The following values of parameters are used: $r(t=0)=1$, $q(t=0)=0$, $A=1.1\times10^{-2}$ s^{-1}, $A_1=6\times10^{-3}$ s^{-1}, $A_2=1\times10^{-4}$ s^{-1}, $A_3=0$, $A_4=1\times10^{-2}$ s^{-1}, $A_5=0$, and $N_s(t=0)=1\times10^{16}$ cm^{-3}. The calculated illumination-time dependence of the dangling bond density is fitted to a power-law function given by

$$N_d(t) = N_d(0)(1 + at^b), \tag{32}$$

with $a=0.154$ and $b=0.397$, as shown in Fig. 14. The fit of

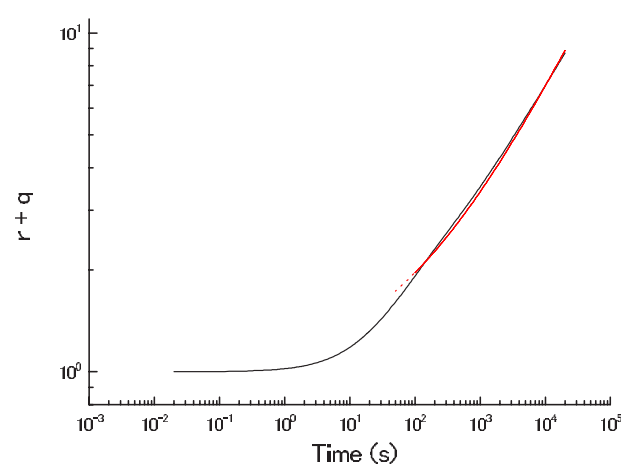

FIG. 14. (Color online) Fitting of calculated curves of $r+q$ vs illumination time (solid lines) by a power-law function given by Eq. (32) (dotted line) for the case of Stutzmann *et al.*

the N_d vs t curve is not too bad in the limited range of t. Thus, the case of $A_4 \neq 0$ ($C_4 \neq 0$) leads us to nonsaturation of the light-induced dangling bond density, as was mentioned before. The above value of b in Eq. (32) is close to that predicted from the weak-bond breaking model by Stutzmann *et al.*,[12] i.e., $b=1/3$.

D. Low-temperature illumination

The light-induced defect creation at low temperatures and its illumination-temperature dependence in a-Si:H are very important to elucidate the mechanism underlying in the light-induced defect creation at room temperature.

The luminescence fatigue, $\Delta I_L/I_L < 0$, i.e., the relative change in the luminescence intensity $\Delta I_L/I_L$, at 4.2 K associated with prolonged illumination by argon-ion laser light at 2.41 eV suggests that dangling bonds are created after prolonged illumination, because they act as nonradiative recombination centers.[68] Further measurements showed that the absolute value of $\Delta I_L/I_L$, i.e., 0.6, obtained after illumination by laser light of 8 W/cm^2 for 1 h at 7 K is comparable to that at 300 K, i.e., 0.4, in standard GD a-Si:H prepared at 300 °C.[68,69] After then, the optically detected magnetic resonance (ODMR) measurements were done at 2 K in standard GD a-Si:H samples prepared at 300 °C using an argon-ion laser of 360 mW at 2.41 eV.[70] To our knowledge, the ODMR measurement presented direct evidence for the light-induced creation of dangling bonds at low temperatures, i.e., the dangling bond signal observed as an ODMR signal, i.e., the so called quenching signal, decreasing the luminescence intensity at resonance, was increased after the illumination by the argon-ion laser light for 30 min at 2 K, monitoring the intensity of emitted light of 1.16 eV. As such, it was concluded from the ODMR measurements at 2 K that a number of dangling bonds being more than native dangling bonds are created by illumination at 2 K. However, the ODMR measurement is inadequate for estimating the spin density. After then, detailed ESR measurements have been carried out to estimate the dangling bond density created by prolonged illumination at low temperatures and its dependence on illumination temperature for high-quality a-Si:H samples.[71–73] The ESR measurement after illumination at 77 K has been done for low-quality a-Si:H samples containing a large amount of hydrogen such as hydrogen content of 30 at. %.[74] The light-induced defect creation at low temperatures has been investigated from the sub-band-gap absorption deduced from the constant photocurrent method.[75] The light-induced defect creation has also been investigated from the luminescence measurements, as mentioned above.

First, we discuss how our model described in Sec. II can be applied to the low-temperature illumination. The hydrogen movement should be slow at low temperatures compared with at room temperature. In our model, the distance between two separate dangling bonds, i.e., a normal dangling bond and a hydrogen-related dangling bond, may be shorter than that for the room temperature illumination, i.e., ~13 Å,[76] as will be shown in the Appendix. Hydrogen is dissociated from a hydrogen-related dangling bond and then terminates a nearby hydrogen-related dangling bond, and consequently two normal dangling bonds are left behind, as illustrated in Fig. 8, where configurations of (a) and (b) transform to those of (c) and (d). A dissociated hydrogen atom moves at a short distance to find a nearby hydrogen-related dangling bond. This means that the distance between those two normal dangling bonds should be short, as shown in Fig. 8. If two hydrogen atoms are dissociated from two nearby hydrogen-related dangling bonds, a hydrogen molecule would be created by collision of those two hydrogen atoms.

The probability that two separate normal dangling bonds are created by illumination depends on the probability that a metastable hydrogen finds a nearby hydrogen-related dangling bond, and on the termination coefficient C_4, as illustrated in Fig. 8. For room temperature illumination, the probability that a metastable hydrogen finds a nearby hydrogen-related dangling bond may be higher than that for low-temperature illumination because the movement distance of a metastable hydrogen atom at room temperature becomes longer than that at low temperature. For low-temperature illumination, hydrogen movement is slow, but the same situation as mentioned above occurs, so that two separate normal dangling bonds of short distance apart are created even for low-temperature illumination. As far as the creation efficiency of two separate dangling bonds, i.e., a normal dangling bond and a hydrogen-related dangling bond, is concerned, it depends on illumination temperature, as will be discussed below.

Second, we discuss the experimental results on the light-induced defect creation at low temperatures and its dependences on illumination temperature obtained so far. Schultz and Taylor[72,73] measured the light-induced dangling bond density as a function of illumination temperature in the range of 65–340 K for high-quality a-Si:H samples using an argon-ion laser of 500 mW/cm^2 at 2.41 eV. From this dependence, the activation energy of 10 meV has been obtained in this temperature range. This activation energy may correspond to that for potential barriers of hydrogen atom associated with its movement necessary for separating two dangling bonds, i.e., a normal dangling bond and a hydrogen-related dangling bond. According to previous studies,[5] the tunneling motion of hydrogen may be dominant below 60 K, while its hopping motion may be dominant above 60 K. Thus, below 60 K, the creation efficiency would be reduced from that at 65 K, considering that the tunneling motion of hydrogen should be slower than the hopping motion of hydrogen. So far, the ESR measurement has not been done to estimate the activation energy below 65 K, although it has been done only at 40 K in the temperature range below 65 K.[71]

However, the illumination-temperature dependence of the light-induced sub-band-gap absorption at 1.25 or 1.35 eV, $\Delta\alpha/\alpha_0$, relative to that before illumination α_0 has been measured in the range of 4.2–300 K.[75] The value of $\Delta\alpha/\alpha_0$ exhibits a broad minimum around 80–150 K. This result disagrees with that obtained from the ESR measurements above 65 K. The sub-band-gap absorption involves ionized dangling bonds as well as neutral dangling bonds, so that the creation efficiency obtained from $\Delta\alpha/\alpha_0$ is not uniquely determined by neutral dangling bonds. Thus, the creation effi-

ciency obtained from the ESR measurement is considered to be more precise than that obtained from the sub-band-gap absorption measurement.

In a previous model,[14–17] we take into account only the light-induced creation process of two separate dangling bonds, i.e., a normal dangling bond and a hydrogen-related dangling bond. However, in the present model, the dissociation process of hydrogen atoms from the hydrogen-related dangling bonds and their termination process to those two types of dangling bonds are taken into account as well. Therefore, the calculated result of C_{SW} defined in Eq. (10) of a paper by Stutzmann *et al.*[12] and given in a previous publication[14,17] should be corrected, taking into account the above dissociation and termination processes. Here, it is noted that C_d in Refs. 14 and 17 is given by $C_{SW}A_t$, where A_t is the rate for recombination of tail electrons with trapped holes in normal and specific weak bonds (weak bond adjacent to a Si-H bond) and is estimated to be 1×10^{-8} cm^3 s^{-1}. Further, the illumination-time dependence of light-induced dangling bond density, ΔN_s, is determined by C_1, C_2, and C_4 as well as C_d for high-quality *a*-Si:H samples for which C_3 is neglected as mentioned before. Thus, the illumination-time dependence of ΔN_s at low temperatures cannot be discussed uniquely in terms of only one or two parameters such as shown in previous papers.[14–17] It is worth noting that ΔN_s is experimentally proportional to t^m where the values of m are 0.55 and 1.5 at 340 and 65 K, respectively.[72] The value of m has also been reported to be 0.33 at room temperature.[12] Quantitative considerations on the illumination-time dependence of ΔN_s at low temperatures are beyond the scope of this paper, so they remain as a future problem.

IV. CONCLUSIONS

It is concluded that a model of light-induced defect creation in *a*-Si:H presented in this paper can account for most of the aspects of experimental results on the kinetics of light-induced dangling bonds under continuous illumination as well as for the qualitative aspects of experimental results for low-temperature illumination. Further investigations on the dispersive parameters of the light-induced defect creation process are useful in elucidating detailed aspects of mechanism for light-induced defect creation in *a*-Si:H.

ACKNOWLEDGMENTS

The authors wish to thank C. Ogihara and K. Takeda for helpful discussions throughout the course of this study. They also acknowledge K. Shimakawa and S. Kugler for useful discussions on experimental and theoretical aspects of light-induced defect creation in *a*-Si:H, respectively.

APPENDIX: DISTANCES BETWEEN HYDROGEN AND DANGLING BOND AND AMONG DANGLING BONDS

Isoya *et al.*[77] and Yamasaki and Isoya[78] concluded that their experiments using electron-spin-echo-envelope modulation (ESEEM) and an instantaneous diffusion of pulsed electron spin resonance (ESR) technique have revealed the following facts: (i) The light-induced dangling bonds as well as the native dangling bonds exist, isolated more than 100 Å apart from other dangling bonds, and (ii) they are formed in the hydrogen-depleted region, being separated from the closest hydrogen atom by a distance of 4.2 Å. We have already pointed out[44] that the proximity of a hydrogen atom to the dangling bond site of the hydrogen-related dangling bond results in a rapid decay of the modulation of ESEEM within the dead time of the spectrometer, so that the presence of hydrogen-related dangling bonds cannot be detected in their ESEEM measurements.

The number of the hydrogen atom located near the dangling bond site is 1 in a hydrogen-related dangling bond, while that of hydrogen atoms increases with increasing their distance from the dangling bond site. This means that the amplitude of the modulation of ESEEM arising from the hydrogen atom located near the dangling bond site becomes weak compared to that arising from hydrogen atoms located far from the dangling bond site. This is also the reason why the former signal (amplitude of ESEEM) is weaker than the latter signal.

Yamasaki and Isoya[78] measured the phase memory curves corresponding to the Fourier transform of the spin packet obtained from the two-pulse Hahn echo ($90°$-τ-$180°$-τ-echo: τ is scanned) measurement. They obtained 3.8×10^{-2} G as the local magnetic field from the phase memory curves for an *a*-Si:H sample containing dangling bonds of 8.4×10^{17} cm^{-3}. The value of 3.8×10^{-2} G corresponds to the average distance of dangling bonds of 100 Å. On the other hand, the value of 1.8–1.9 G for a half of full width at half maximum (FWHM) has been estimated from the deconvolution of ESR spectra[76] measured at 434 MHz by Brandt *et al.*[79] For a high-quality *a*-Si:H sample of $N_d = 2 \times 10^{15}$ and 2×10^{16} cm^{-3} corresponding to before and after light soaking, Yamasaki and Isoya[78] further concluded that the dangling bonds are separated from each other by more than 100 Å on the average. Such a large discrepancy in the value of the local magnetic field seems to us to arise from different types of measurements. According to Yamasaki and Isoya,[78] the instantaneous spin diffusion due to dipolar interaction determines the phase memory curve for low-quality samples, while the spin diffusion via hyperfine interaction between the dangling bond electron spin and the matrix nuclear spin does the phase memory curve for high-quality samples. For both cases, the spin diffusion process should be treated, taking into account the distribution of dangling bond electron spins. This is a sort of stochastic processes in a disordered system, pursuing the time evolution of dangling bond electron spin. Yamasaki and Isoya[78] took the average value of the dipolar field taking into account random distribution of dangling bonds. We think that this procedure may not be justified in such a dynamical process.

For the static process, e.g., the linewidth due to the dipolar interaction between dangling bond electron spins, one can employ the moment method by Van Vleck[80] to treat the linewidth. Kittel and Abrahams[81] calculated the linewidth due to the dipolar interaction of spins distributed at random. The average second moment of dipolar interaction, $\langle \Delta H^2 \rangle_{\mathrm{av}}$, is given by

$$\langle \Delta H^2 \rangle_{\rm av} = [S(S+1)/3N] \sum_{j,k}{}' B_{jk}^2, \quad \text{(A1)}$$

where N is the actual number of magnetic species and the summation is performed over all occupied sites ($j \neq k$). B_{jk} is given by

$$B_{jk} = -(3/2) g \mu_B r_{jk}^{-3} (3 \cos^2 \theta_{jk} - 1), \quad \text{(A2)}$$

where g and μ_B are the g value of dangling bonds (the difference in the g value between two types of dangling bonds is neglected) and the Bohr magneton, respectively, and θ_{jk} is the angle between the vector $\mathbf{r}_{jk}$ and the static magnetic field. However, it is not guaranteed that dangling bond electron spins are distributed homogeneously at random.

Now, we take a model of light-induced defect creation in a-Si:H described in this paper, i.e., there is a close pair of a normal dangling bond and a hydrogenrelated dangling bond or two neighboring normal dangling bonds. The intradistance within a close pair, r, and the site of a dangling bond, e.g., a normal dangling bond, are fixed, and then it is assumed that the site of another dangling bond, i.e., either a normal dangling bond or a hydrogen-related dangling bond, is randomly distributed over the spherical surface of radius r, but only one magnetic species, i.e., either a normal dangling bond or a hydrogen-related dangling bond exists on this spherical surface. Based on the above distribution of magnetic species, FWHM due to dipolar interaction between magnetic species has been calculated[76] using the moment method by Van Vleck.[80] The result is summarized below. The average second moment of dipolar interaction, $\langle \Delta H^2 \rangle_{\rm av}$, is calculated by performing the statistical average on the spherical surface of radius r. Then, we obtain

$$\langle \Delta H^2 \rangle_{\rm av} = (9/20) g^2 \mu_B^2 r^{-6} = (9/20) A^2, \quad \text{(A3)}$$

$$A = g \mu_B r^{-3} \text{ (in gauss)}. \quad \text{(A4)}$$

The fourth moment of dipolar interaction is given by Eq. (21) in Ref. 80. Its average is calculated as follows:

$$\langle \Delta H^4 \rangle_{\rm av} = (3627/2800) A^4. \quad \text{(A5)}$$

As shown below, we take a Lorentzian line shape with cutoff fields $H_0 \pm \alpha$ and half-width at half maximum Γ. The second and fourth moments are given by

$$\langle \Delta H^2 \rangle_{\rm av} = 2\Gamma \alpha / \pi, \quad \text{(A6)}$$

$$\langle \Delta H^4 \rangle_{\rm av} = 2\Gamma \alpha^3 / 3\pi. \quad \text{(A7)}$$

The ratio of the average second moment to the average fourth moment is

$$\langle \Delta H^2 \rangle_{\rm av} / \langle \Delta H^4 \rangle_{\rm av} = 3\alpha^{-2}. \quad \text{(A8)}$$

In our case, this ratio is $0.347/A^2$, so that we obtain $\alpha = 2.94A$. Then, the FWHM is given by

$$\text{FWHM} = 2\Gamma = \langle \Delta H^2 \rangle_{\rm av} \pi / \alpha = (9/20) A \pi / 2.94. \quad \text{(A9)}$$

If we take the values of Γ, 1.8 and 1.9 G, obtained from the deconvolution of ESR spectra[76] measured at 434 MHz for glow-discharge a-Si:H samples ([H]=10 at. %) by Brandt *et al.*,[79] we obtain $r \cong 13.5$ and 13.3 Å, respectively.

According to Abragam[82] and Kittel and Abrahams,[81] if the conditions $f < 0.01$ (the fraction of the occupied site) and $\langle \Delta H^4 \rangle_{\rm av} / \langle \Delta H^2 \rangle_{\rm av^2} \gg 3$ are satisfied, the line shape is approximated by a truncated Lorentzian curve. Although the condition has been applied to the case of a magnetically diluted system in the regular cubic crystal lattice, we assume that this condition is also applicable to our case. In our case, f is estimated as follows: A magnetic species occupies a site on the spherical surface of radius r, i.e., 13 Å. The total number of the sites on the sphere is estimated from dividing the surface area by the area occupied by one site, i.e., (2.35 Å)^2, that is 384 sites. Thus, we obtain $f = 2.6 \times 10^{-3}$. Further, we obtain $\langle \Delta H^4 \rangle_{\rm av} / \langle \Delta H^2 \rangle_{\rm av^2} = 6.38$ from Eqs. (A6) and (A7). Thus, the above conditions are satisfied, so that the line shape is approximated by a truncated Lorentzian curve. As such, the truncated Lorentzian curve that we use in the above consideration is justified.

In the above consideration, we neglected a distribution of r. The value of r is obviously distributed over some range. However, the distribution is considered to be narrow in the light of our model, so that the value of r is approximately fixed.

From the above consideration, it is concluded that the close pairs of dangling bonds 13 Å apart reasonably account for the spin-packet width of 1.8–1.9 G. Furthermore, it is noted that the existence of close pairs of dangling bonds is in contrast with the assumption of randomly distributed dangling bonds by Isoya *et al.*[77] and Yamasaki and Isoya.[78] Finally, we would like to add that the inhomogeneous distribution of light-induced dangling bonds has been suggested from frequency-resolved spectroscopy measurements on luminescence in a-Si:H by Ogihara *et al.*[83]

*Present address: C-305 Wakabadai 2-12, Inagi, Tokyo 206-0824, Japan; k.morigaki@yacht.ocn.ne.jp
†hhikita@meikai.ac.jp

[1] D. L. Staebler and C. R. Wronski, Appl. Phys. Lett. **31**, 292 (1977).
[2] K. Shimakawa, A. Kolobov, and S. R. Elliott, Adv. Phys. **44**, 475 (1995).
[3] H. Fritzsche, *Amorphous Silicon Technology*, MRS Symposia Proceedings No. 467 (Materials Research Society, Pittsburgh, 1997), p. 19.
[4] M. Stutzmann, *Amorphous Silicon Technology*, MRS Symposia Proceedings No. 467 (Materials Research Society, Pittsburgh, 1997), p. 37.
[5] K. Morigaki, *Physics of Amorphous Semiconductors* (World Scientific, Singapore/Imperial College Press, London, 1999).
[6] H. Fritzsche, Annu. Rev. Mater. Res. **31**, 47 (2001).

[7] J. Singh and K. Shimakawa, *Advances in Amorphous Semiconductors* (Taylor & Francis, London, 2003).
[8] T. Shimizu, Jpn. J. Appl. Phys., Part 1 **43**, 3257 (2004).
[9] I. Hirabayashi, K. Morigaki, and S. Nitta, Jpn. J. Appl. Phys. **19**, L357 (1980).
[10] J. I. Pankove and J. E. Berkeyheiser, Appl. Phys. Lett. **37**, 705 (1980).
[11] H. Dersch, J. Stuke, and J. Beichler, Appl. Phys. Lett. **38**, 456 (1981).
[12] M. Stutzmann, W. B. Jackson, and C. C. Tsai, Phys. Rev. B **32**, 23 (1985).
[13] F. Yonezawa, S. Sakamoto, and M. Hori, J. Non-Cryst. Solids **137&138**, 135 (1991).
[14] K. Morigaki, Jpn. J. Appl. Phys., Part 1 **27**, 163 (1988).
[15] K. Morigaki, Jpn. J. Appl. Phys., Part 2 **28**, L2128 (1989).
[16] K. Morigaki, Jpn. J. Appl. Phys., Part 2 **29**, L1582 (1990).
[17] K. Morigaki, J. Non-Cryst. Solids **141**, 166 (1992).
[18] K. Morigaki and H. Hikita, Solid State Commun. **114**, 69 (2000).
[19] K. Morigaki and H. Hikita, J. Non-Cryst. Solids **266-269**, 410 (2000).
[20] K. Morigaki and H. Hikita, *Proceedings of the 25th International Conference on the Physics of Semiconductors* (Springer, Berlin, 2000), p. 1485.
[21] K. Morigaki and H. Hikita, J. Non-Cryst. Solids **299-302**, 455 (2002).
[22] K. Morigaki, H. Hikita, H. Takemura, T. Yoshimura, and C. Ogihara, Philos. Mag. Lett. **83**, 341 (2003).
[23] D. E. Carlson, Appl. Phys. A: Solids Surf. **A41**, 305 (1986).
[24] C. Godet and P. Roca i Cabarrocas, J. Appl. Phys. **80**, 97 (1996).
[25] C. Godet, J. Non-Cryst. Solids **227-230**, 272 (1998).
[26] C. Godet, Philos. Mag. B **77**, 765 (1998).
[27] H. M. Branz, Solid State Commun. **105**, 387 (1998).
[28] H. M. Branz, Phys. Rev. B **59**, 5498 (1999).
[29] H. M. Branz, J. Non-Cryst. Solids **266-269**, 391 (2000).
[30] H. M. Branz, Sol. Energy Mater. **78**, 425 (2003).
[31] C. Longeaud, D. Roy, and O. Saadane, Phys. Rev. B **65**, 085206 (2002).
[32] C. Ogihara, H. Takemura, T. Yoshimura, and K. Morigaki, J. Non-Cryst. Solids **299-302**, 637 (2002).
[33] K. Morigaki, Jpn. J. Appl. Phys., Part 2 **27**, L138 (1988).
[34] K. Takeda, H. Hikita, Y. Kimura, H. Yokomichi, M. Yamaguchi, and K. Morigaki, Jpn. J. Appl. Phys., Part 1 **36**, 991 (1997).
[35] S. Vignoli, R. Meudre, M. Meudre, P. Roca i Cabarrocas, C. Godet, and P. Morin, J. Non-Cryst. Solids **198-200**, 474 (1996).
[36] R. A. Street, Physica B **170**, 69 (1991).
[37] W. B. Jackson and C. C. Tsai, Phys. Rev. B **45**, 6564 (1992).
[38] P. Kleider, C. Longeaud, and P. Roca i Cabarrocas, J. Non-Cryst. Solids **164-166**, 403 (1993).
[39] S. J. Jones, Y. Chen, D. L. Williamson, U. Kroll, and P. Roca i Cabarrocas, J. Non-Cryst. Solids **164-166**, 131 (1993).
[40] P. Morin and P. Roca i Cabarrocas, *Amorphous Silicon Technology*, MRS Symposia Proceedings No. 336 (Materials Research Society, Pittsburgh, 1994), p. 281.
[41] H. Yokomichi and K. Morigaki, Solid State Commun. **63**, 629 (1987).
[42] H. Yokomichi, I. Hirabayashi, and K. Morigaki, Solid State Commun. **61**, 697 (1987).
[43] H. Yokomichi and K. Morigaki, Solid State Commun. **85**, 759 (1993).
[44] H. Yokomichi and K. Morigaki, Philos. Mag. Lett. **73**, 283 (1996).
[45] H. Hikita, K. Takeda, Y. Kimura, H. Yokomichi, and K. Morigaki, J. Phys. Soc. Jpn. **66**, 1730 (1997).
[46] K. Morigaki, H. Hikita, M. Yamaguchi, and Y. Fujita, J. Non-Cryst. Solids **227-230**, 338 (1998).
[47] O. Astakhov, F. Finger, R. Carius, A. Lambertz, Y. Petrusenko, V. Borysenko, and D. Barankov, J. Non-Cryst. Solids **352**, 1020 (2006).
[48] H. Hikita, K. Takeda, H. Yokomichi, and K. Morigaki (unpublished).
[49] B. B. Nielsen, P. Johannesen, P. Stallinga, K. B. Nielsen, and J. R. Byberg, Phys. Rev. Lett. **79**, 1507 (1997).
[50] T. Su, S. Chen, P. C. Taylor, R. S. Crandall, and A. H. Mahan, Phys. Rev. B **62**, 12849 (2000).
[51] P. A. Fedders, D. J. Leopold, P. H. Chan, R. Borzi, and R. E. Norberg, Phys. Rev. Lett. **85**, 401 (2000).
[52] C. G. Van de Walle and B. Tuttle, *Amorphous Silicon Technology*, MRS Symposia Proceedings No. 557 (Materials Research Society, Pittsburgh, 1999), p. 275.
[53] S. Zukotynski, F. Gaspari, N. Kherani, T. Kosteski, K. Law, W. T. Shmayda, and C. M. Tan, J. Non-Cryst. Solids **299-302**, 476 (2002).
[54] H. R. Park, J. Z. Liu, and S. Wagner, Appl. Phys. Lett. **55**, 2658 (1989).
[55] M. Isomura, N. Hata, and S. Wagner, J. Non-Cryst. Solids **137&138**, 223 (1991).
[56] M. Isomura, N. Hata, and S. Wagner, *Amorphous Silicon Technology*, MRS Symposia Proceedings No. 219 (Materials Research Society, Pittsburgh, 1991), p. 27.
[57] Z. Y. Wu, J. M. Siefert, and B. Equer, J. Non-Cryst. Solids **137&138**, 227 (1991).
[58] M. Stutzmann, M. C. Rossi, and M. S. Brandt, Phys. Rev. B **50**, 11592 (1994).
[59] C. Godet, P. Morin, and P. Roca i Cabarrocas, J. Non-Cryst. Solids **198&200**, 449 (1996).
[60] D. Redfield and R. H. Bube, Appl. Phys. Lett. **54**, 1037 (1989).
[61] D. Redfield, *Amorphous Silicon Technology*, MRS Symposia Proceedings No. 258 (Materials Research Society, Pittsburgh, 1992), p. 341.
[62] W. B. Jackson, *Amorphous Silicon Technology*, MRS Symposia Proceedings No. 149 (Materials Research Society, Pittsburgh, 1989), p. 571.
[63] W. B. Jackson and J. Kakalios, Phys. Rev. B **37**, 1020 (1988).
[64] Y. Poissant, P. St'ahel, and P. Roca i Cabarrocas, *Proceedings of the European Photovoltaic Solar Energy Conference and Exhibition*, (James & James Science, London, 2000), p. 377.
[65] K. Shimakawa, Meherun-Nessa, H. Ishida, and A. Ganjoo, Philos. Mag. **84**, 81 (2004).
[66] J. Kakalios, R. A. Street, and W. B. Jackson, Phys. Rev. Lett. **59**, 1037 (1987).
[67] K. Morigaki and F. Yonezawa, J. Non-Cryst. Solids **164-166**, 215 (1993).
[68] K. Morigaki, I. Hirabayashi, M. Nakayama, S. Nitta, and K. Shimakawa, Solid State Commun. **33**, 851 (1980).
[69] M. Yoshida and K. Morigaki, J. Phys. Soc. Jpn. **59**, 1733 (1990).
[70] K. Morigaki, Y. Sano, and I. Hirabayashi, J. Phys. Soc. Jpn. **51**, 147 (1982).
[71] M. Yoshida and P. C. Taylor, *Amorphous Silicon Technology*, MRS Symposia Proceedings No. 258 (Materials Research Society, Pittsburgh, 1992), p. 347.

[72] N. Schultz and P. C. Taylor, *Amorphous Silicon Technology*, MRS Symposia Proceedings No. 557 (Materials Research Society, Pittsburgh, 1999), p. 353.
[73] N. Schultz and P. C. Taylor, *Amorphous and Microcrystalline Silicon Technology*, MRS Symposia Proceedings No. 609 (Materials Research Society, Pittsburgh, 2000), p. A3.4.1.
[74] I. Hirabayashi, K. Morigaki, and M. Yoshida, Sol. Energy Mater. **8**, 153 (1982).
[75] P. Stradins and H. Fritzsche, Philos. Mag. B **69**, 121 (1994).
[76] K. Morigaki and H. Hikita, Res. Bull. Hiroshima Inst. Tech. **33**, 135 (1999).
[77] J. Isoya, S. Yamasaki, H. Okushi, A. Matsuda, and K. Tanaka, Phys. Rev. B **47**, 7013 (1993).
[78] S. Yamasaki and J. Isoya, J. Non-Cryst. Solids **164-166**, 169 (1993).
[79] M. S. Brandt, M. W. Bayerl, M. Stutzmann, and C. F. O. Graeff, J. Non-Cryst. Solids **227-230**, 343 (1998).
[80] J. H. Van Vleck, Phys. Rev. **74**, 1168 (1948).
[81] C. Kittel and E. Abrahams, Phys. Rev. **90**, 238 (1953).
[82] A. Abragam, *The Principles of Nuclear Magnetism* (Clarendon, Oxford, 1961).
[83] C. Ogihara, T. Nomiyama, H. Yamamoto, K. Nakanishi, J. Harada, X. Yu, and K. Morigaki, J. Non-Cryst. Solids **352**, 1064 (2006).